Numerical investigation of energy potential and performance of a residential building-integrated solar micro-CHP system

Simon Martinez, Ghislain Michaux, Patrick Salagnac, Jean-Luc Faure

NUMERICAL INVESTIGATION OF ENERGY POTENTIAL AND PERFORMANCE OF A RESIDENTIAL BUILDING-INTEGRATED SOLAR μCHP SYTEM

Simon Martinez[1]*, Ghislain Michaux[1], Patrick Salagnac[1], Jean-Luc Faure[2]

(1) LaSIE, UMR-CNRS 7356, Université de La Rochelle, av. Michel Crépeau, 17 042 la Rochelle Cedex 1, France

(2) Département de Génie Civil, Faculté des Sciences et Technologie, Université de La Rochelle, av. Michel Crépeau, 17 042 la Rochelle Cedex 1, France

1. ABSTRACT

The studied micro-CHP unit converts concentrated solar energy into electricity and heat by coupling a 46.5 m² parabolic trough collector with an oil-free single-cylinder steam engine operating according to the Hirn cycle. Originalities of this system are two axis solar tracking and direct steam generation. The exhaust heat of the cycle is recovered to cover building's heat needs, while the electricity is either self-consumed or fed back into the electricity grid. Experimental studies have shown that it is impossible to achieve continuous operation of the facility without an additional heat source. Thus, we are studying solutions for integrating a backup heating system from dynamic thermal simulations performed with TRNSYS© software One of them consists in adding a 30 kW boiler to the primary circuit in order to ensure daily electricity production. However, this is restricted by the considered storage tank. A parametric study on the volume of the storage tank makes it possible to propose an optimal solution for heat recovery. The results indicate that a storage volume of 3 m^3 meets the needs of the building and limits the heat losses due to heat storage. In order to optimize the use of such a micro-CHP unit, a heat sharing between several buildings equipped with 3 m^3 storage seems therefore to be a coherent solution.

Keywords: micro-CHP, distributed generation, solar energy, concentrating solar power, direct steam generation, building, numerical simulation

2. INTRODUCTION

Micro-CHP is a distributed generation of electricity and heat for low electrical power (<50 kWel) [1] [2]. The principle is to recover waste heat during electrical production using a thermodynamic cycle. This heat can then be used to cover heating and domestic hot water needs of a building.

Micro-CHP reduces primary energy consumption and greenhouse gas emissions with higher efficiency than separate production of electricity and heat [3]. It should also be noted that in Europe, the recent "Climate Energy Package" agreements signed in 2014 aim to increase renewable energies in the energy mix by up to 27 %, reduce greenhouse gas emissions by at least 40 % and improve the energy efficiency of systems by at least 27 % by 2030 [4]. A micro-CHP unit operating from concentrated solar energy can therefore meet the objectives previously mentioned. In this context of integrating renewable energies into the energy mix and improving the efficiency of energy production systems, many micro-CHP units using renewable energies are currently under study [5].

The solar micro-CHP unit studied here converts concentrated solar energy into electricity and heat by coupling a 46.5 m² parabolic trough collector with an oil-free single-cylinder steam

engine operating according to a Hirn cycle. This system has been the subject of several previous works [6] [7] [8] dealing with the evaluation of performances of the solar concentrator, the steam engine and the whole system. Experimental studies have shown that it is impossible to ensure continuous operation of the installation without an additional heat source [9].

Studies on the integration of micro-CHP units into buildings have already been conducted. Concerning a SenerTech's DACH micro-CHP unit, Campos-Celador *et al.* [10] proposed a thermo-economic study of the integration into a 160 kW boiler room supplying a group of residential buildings. Thanks to annual simulations carried out with TRNSYS16© software, the building's needs have been determined. From a comprehensive study [11], it is possible to define the main advantages and difficulties of integrating a micro-CHP unit into a boiler room. Interesting notions about thermal storage to ensure a continuous electrical production have been highlighted.

Habibi and Varmazyar [10] have conducted an experimental study in order to investigate the behavior of a gas micro-CHP unit generating 14 kW electrical power and 35 kW thermal power. Authors pointed out the influence of heating network's supply temperature to ensure the performance of the installation. The lower the supply temperature is, the better the performance of the system is. It also appeared that an increase in the electrical power generated leads to better overall performances.

For an installation using biofuel, Chen *et al.* [12] proposed a dynamic optimization of an electrical storage installation to meet the electricity and heat needs of a residential building. The originality of this study is installation controlled by a decision tree. However, uncertainties about the performance of the engine powered by biofuel remain under investigation.

In general, it seems that there is a real enthusiasm for micro-cogeneration systems integrated into the building. Several studies [13] [14] [15] [16] and policy proposals [17] [18] illustrate the interest on cogeneration, and specifically micro-cogeneration in buildings [19] [20] [21] [22] [23].

3. SOLAR-MICRO CHP UNIT MODEL

In this section, we describe the main components of the studied solar micro-CHP unit as well as the models used to simulate its operation. For additional technical information on these various components, one can refer to published experimental works previously mentioned.

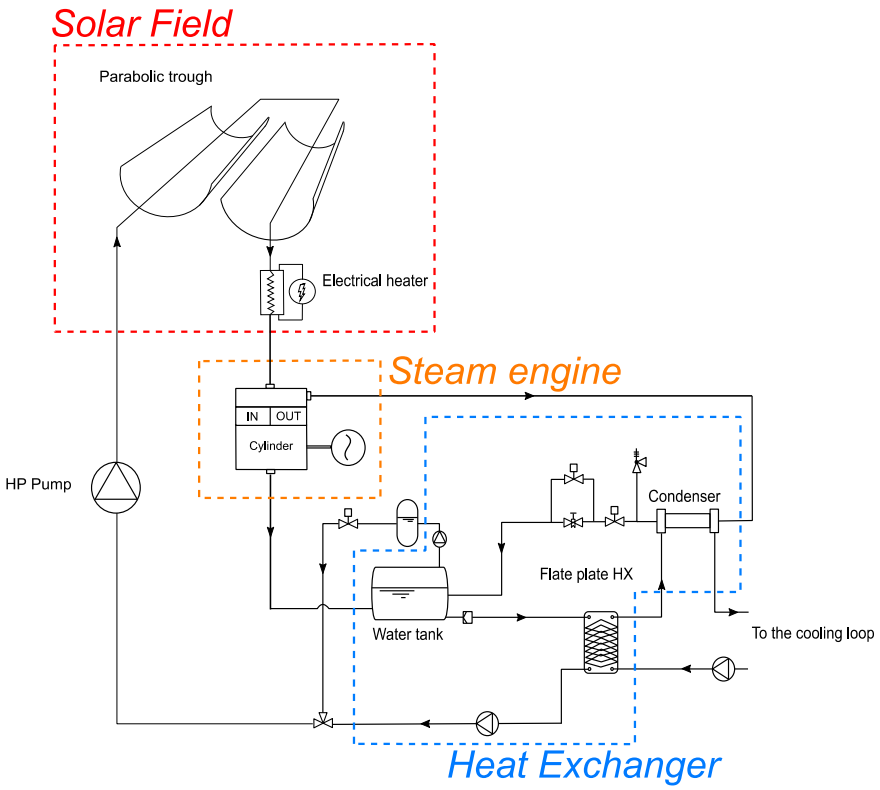

Figure 1 : Schematic diagram of the studied solar micro-CHP unit

Two lines of parabolic trough collectors with a collection area of 46,5 m² following the solar position thanks to a two-axis tracking system compose the solar field. Within the steel absorber tube located at the focal point of the mirror, water circulates at low flow and high pressure to be vaporized. An additional electrical heater ensures good engine intake conditions even in order to compensate solar intermittencies (5 kW). The steam engine converts thermal energy into electrical one using an alternator. The hydraulic skid called « heat exchanger » in Figure 1 is composed by various components providing the interface between the primary loop and a cooling one. Finally, a high pressure pump is used to reach pressure and flowrate set points (25 bars and 30 kg/hr respectively).

3.1 Parabolic trough collector model

A model to characterize the efficiency of the solar concentrator has been defined. It consists of determining the optical efficiency and the convective loss coefficient. Thus, ratio of thermal energy transmitted to the fluid divided per total solar energy received by the mirrors surface can be calculated:

$$\eta_{sol} = \frac{P_{th,sol}}{P_{tot,sol}} = \frac{\dot{m}(h_{out,sol} - h_{in,sol})}{S_{sol} I} = 0.60 - 0.81 \left(\frac{\left(\frac{T_{sat} + T_{in,sol}}{2} \right) - T_{ext}}{I} \right) \quad (1)$$

Where, $\dot{m}$ corresponds to the mass flow in the concentrator, $h_{out,sol}$ is the enthalpy at the outlet of the solar field, $h_{in,sol}$ is the enthalpy at the inlet of the solar field, S_{sol} corresponds to the surface of the mirrors, I corresponds to the irradiance, T_{sat} is the saturation temperature, $T_{in,sol}$ is the water temperature at the inlet of the solar field and T_{ext} represents the external temperature

This polynomial form of efficiency is usually defined for solar thermal systems [24]. Note that an accurate description of direct steam generation generally leads to more complex models [25] [26] [27] [28] that are incompatible with dynamic thermal modelling.

3.2 Steam engine model

The model used for the steam engine has also been based on experimental data obtained on a test bench with a controllable heat source [8]. This model allows to express the filling factor as well as the isentropic efficiency of the engine as a function of the pressure ratio, the intake water density and the engine rotation speed [29] :

$$FF = \sum_{i=0}^{n-1}\sum_{j=0}^{n-1}\sum_{k=0}^{n-1} b_{ijk} \ln(r_p)^i \rho_{in}^j \ln(N)^k + b_{n00} \ln(r_p)^n + b_{0n0} {\rho_{in}}^n + b_{0n0} \ln(N)^n \quad (2)$$

$$\eta_{\exp} = \sum_{i=0}^{n-1}\sum_{j=0}^{n-1}\sum_{k=0}^{n-1} a_{ijk} \ln(r_p)^i \rho_{in}^j N^k + a_{n00} \ln(r_p)^n + a_{0n0} {\rho_{in}}^n + a_{0n0} N^n \quad (3)$$

Where, r_p corresponds to the pressure ratio between the intake and exhaust of the engine, N is the rotational speed of the engine, ρ_{in} is the density at the intake and the coefficients a and b are calibrated from experimental measurements.

In practice, only the first order terms are considered. Once the motor characteristics have been determined, it is possible to calculate the enthalpy of the output fluid as well as the electric production thanks to the following relations:

$$FF = \frac{\dot{m}_{admis}}{\rho_{in}\dot{V}_{swept}} = \frac{\dot{m}_{admis}}{\rho_{in}\left(\frac{N}{60}\right)V_{swept}} \quad (4)$$

$$\eta_{\exp} = \frac{P_{el}}{\dot{m}_{admis}(h_{in} - h_{out,is})} \quad (5)$$

Where P_{el} corresponds to the electrical power, $\dot{m}_{admis}$ is the actual flowrate admitted into the steam engine, V_{swept} is the volume swept by the piston, h_{in} corresponds to the admission steam enthalpy and $h_{out,is}$ is the isentropic steam enthalpy at the outlet of the steam engine.

As described in equation (4), the filling factor therefore corresponds to the ratio of the mass admitted into the engine to the theoretical mass contained in the intake volume.

A stationary balance assuming constant exchange efficiency models heat exchanges between the primary and secondary loops. In accordance with the experimental data, it is assumed that the water flow temperature to the solar field is fixed. Thus, one can write:

$$\begin{aligned} P_{HX} &= \dot{m}(h_{in,HX} - h_{out,HX}) \\ &= \frac{P_{cooling}}{\varepsilon_{HX}} = \frac{\dot{m}_{cooling} C_p (T_{out,cooling} - T_{in,cooling})}{\varepsilon_{HX}} \end{aligned} \quad (6)$$

The efficiency of the exchanger, ε_{HX}, is assumed constant and equal to 80 %. Thus, the thermal power obtained on the secondary loop is deduced from an enthalpy balance and is about 15 kW, which is in agreement with measured experimental values.

3.3 Boiler model

The used model here, defined by its overall efficiency and its combustion efficiency, is a model available in the TRNSYS© TESS library (Type 638). The maximum boiler power output is fixed and the power required to reach the enthalpy set point at the boiler outlet is calculated by:

$$\dot{Q}_{needed} = \dot{m}(h_{obj} - h_{out,PTC}) \tag{7}$$

Where h_{obj} corresponds to the enthalpy aimed at the inlet of the steam engine and $h_{out,PTC}$ corresponds to the enthalpy at the outlet of the solar field.

Once the necessary power is determined, the boiler power output can be defined as follows:

$$\dot{Q}_{boiler} = \min(\dot{Q}_{needed}, \dot{Q}_{\max}) \tag{8}$$

For the boiler model, a total efficiency of 0.78 is defined. The value of the combustion efficiency is 0.85.

3.4 Other models

Pump and hot water tank models come from the TRNSYS library (Type 114 and Type 534 respectively).

4. THE BUILDING MODEL

The building model has been carefully defined because it determine heating requirements according to the envelope, indoor temperature set point, outdoor temperature and internal gains.

4.1 Description

The modelled building is located on the INCAS platform of the INES site located in Chambéry, France. It is a two floors house with a net floor area of 97.5 m². It includes a kitchen, a dining room / living room, a laundry room, an entrance hall and a toilet on the ground floor. On the first floor, there are three bedrooms, a bathroom and a toilet. For the modelling, we consider the following rooms as heated: the bathroom, the kitchen/living room, and the three bedrooms upstairs. Plans of the INCAS house are provided by Figure 2.

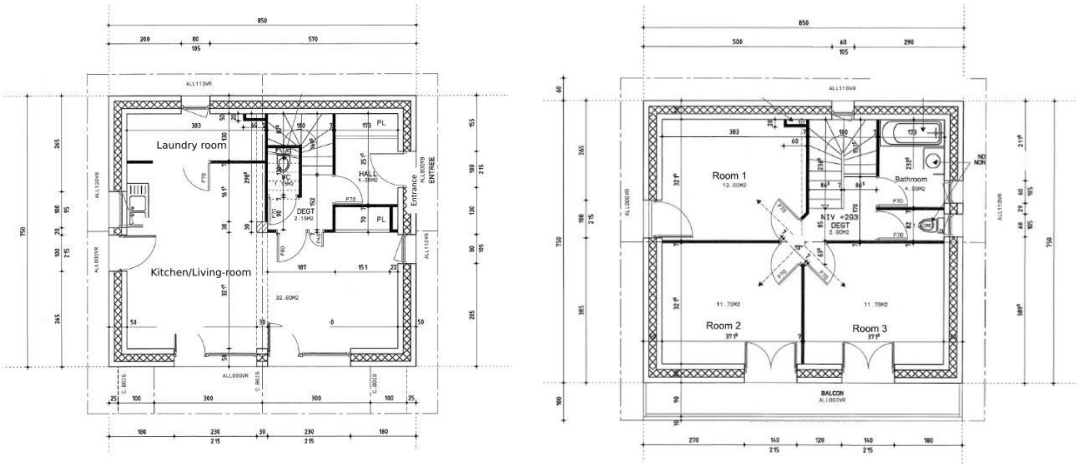

Figure 2: Plans of the INCAS house, ground floor (left) and first floor (right)

4.2 Building heating

The heating contribution of the micro-CHP unit has to ensure the thermal comfort into the house. Thus, set point temperatures are defined in each heated room. Figure 3 shows temperature profiles defined for weekdays and weekends. These temperature levels are essential for calculating losses and heating requirements.

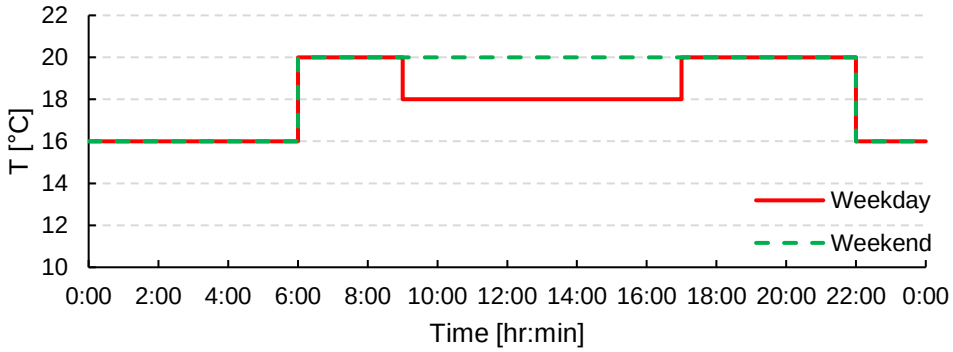

Figure 3 : Set temperatures in heated rooms of the building

Therefore, the heat requirements of the building can be calculated from dynamic thermal simulations performed with TRNSYS© software. For one year, Figure 4 shows the heating capacity required to reach the set point temperature in the heated zones.

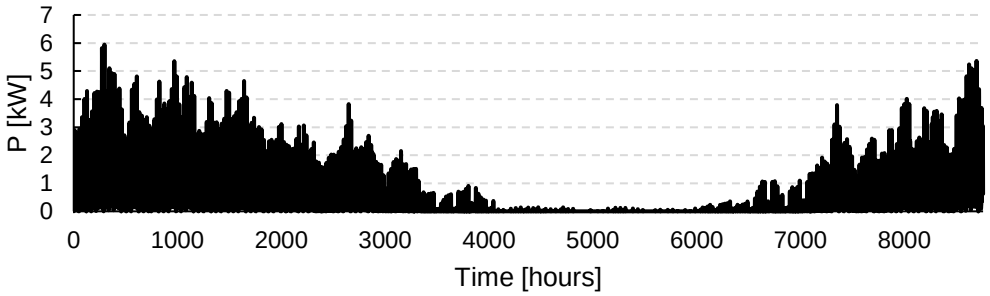

Figure 4 : Annual power profile for heating

4.3 Withdrawal of domestic hot water

The domestic hot water drawing profile is defined for one week and is derived from the open access model developed by McKenna *et al.* [30]. The profile shown by Figure 5 is representative of a consumption of four people. Water is assumed to be consumed at 60°C.

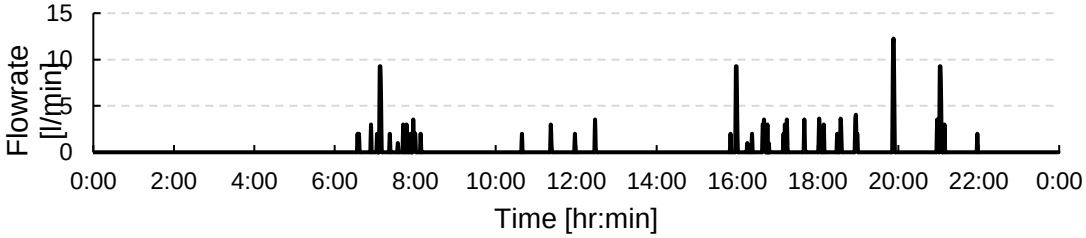

Figure 5: Hot domestic water withdrawal profile

4.4 Electrical requirements

Electrical requirements are based on the McKenna's model [30]. The electricity consumption profile is defined for one day and four occupants. This profile provides the electrical power

consumed by the building (Figure 6). Note that the model distinguishes electrical consumption from lighting and household appliances. Total consumption is considered in this study.

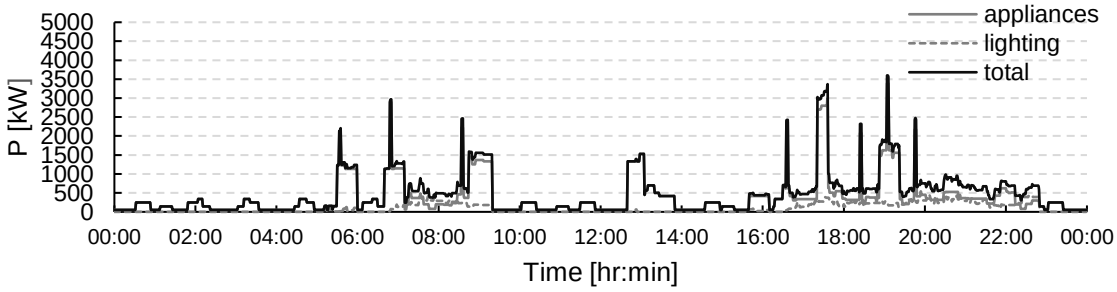

Figure 6: Daily electrical power consumption

5. INTEGRATION OF MICRO-CHP UNIT INTO THE BUILDING

We propose in this numerical work to replace the electrical heater at the solar field outlet by a boiler of greater power (30 kW) in order to ensure the water evaporation even in the absence of sunlight. For the modeling considered, the time step used is 15 min. It results from a compromise between the need for a small time step to represent the control of the micro-generator and a large time step to perform annual reviews. Figure 7 presents a schematic diagram of the coupling between the micro-CHP unit and the building.

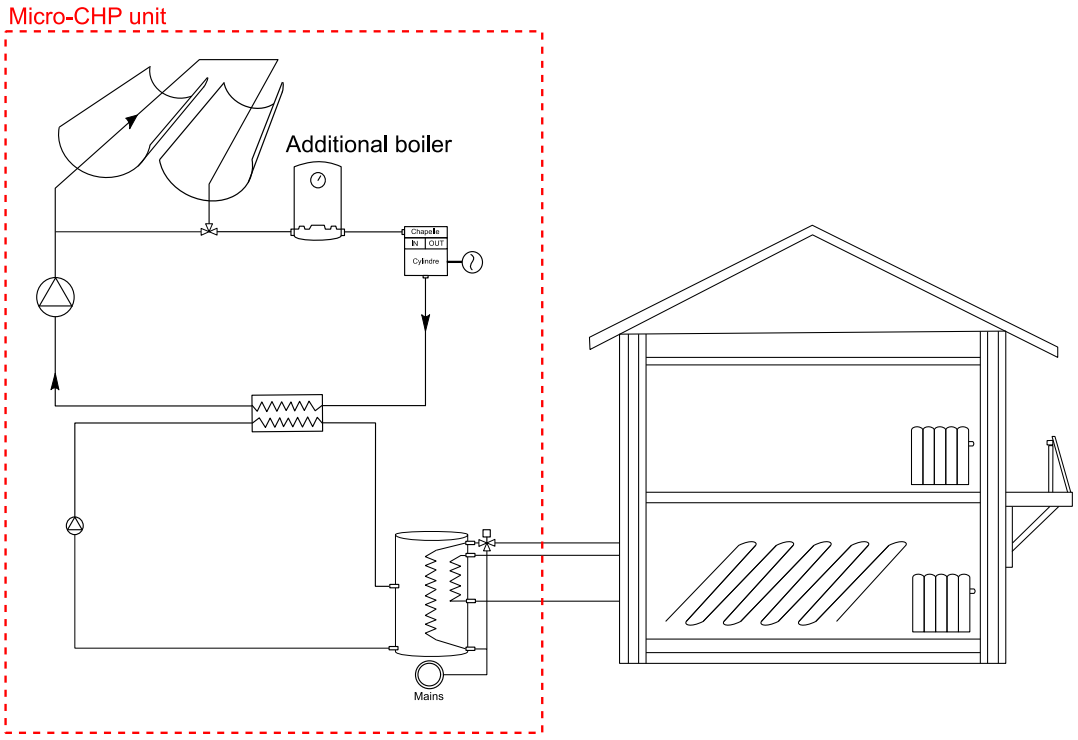

Figure 7: Coupling between the micro-CHP unit and the building

According to the numerical modeling, the micro-CHP unit produces electricity and stores heat in the storage tank regardless of the amount of sunlight, and this in order to provide heating and domestic hot water production for the building.

The objective of this integration is to produce electricity and heat in order to cover building's needs while promoting the use of solar energy. For this purpose, it is assumed that the system operates during the day and as long as the storage tank is not fully charged (average storage tank temperature below 85 °C).

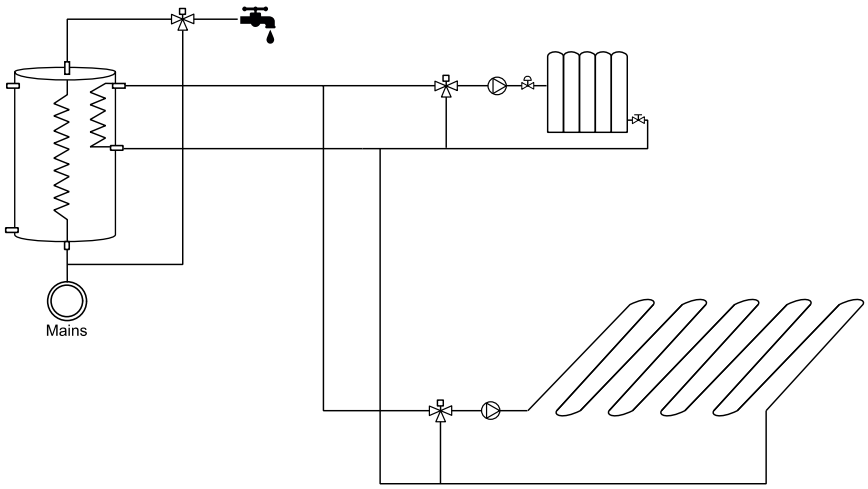

Figure 8: Hydraulic diagram corresponding to the case study

Figure 8 shows the domestic hot water, radiator and underfloor heating distribution networks. For each circuit, solenoid valves ensure the flow temperature of the circuits according to a heating curve.

In this section, we present the architecture of the TRNSys modelling. This study is based on the modelling of the micro-CHP unit, its hydraulic integration and the building.

5.1 The primary loop

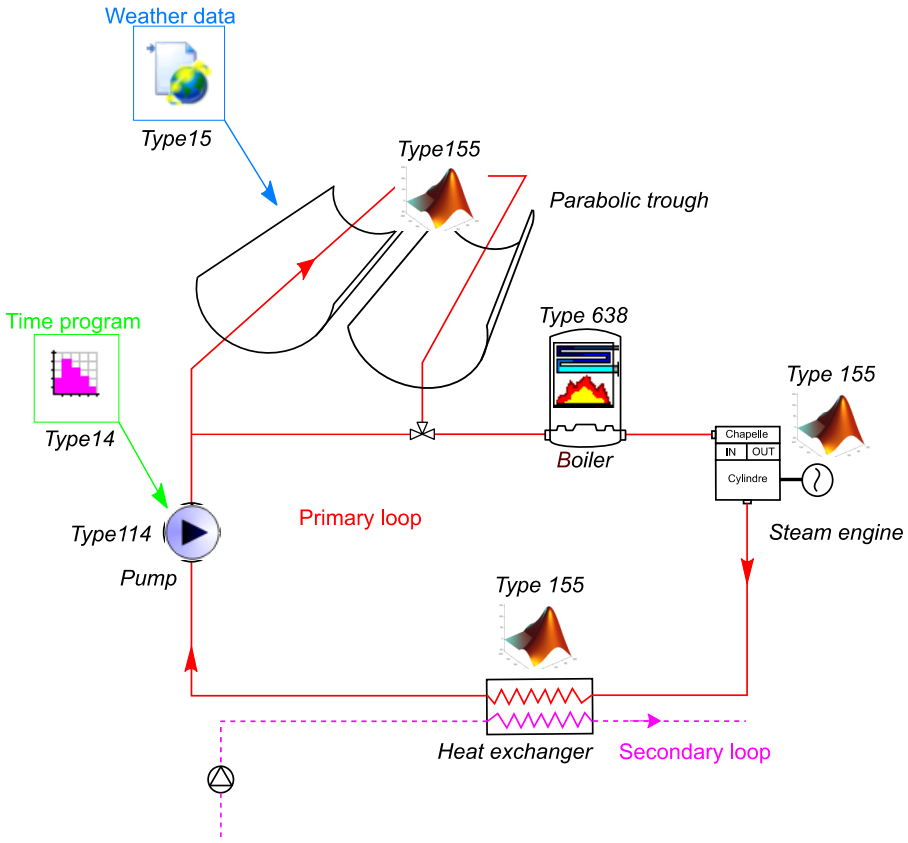

Figure 9: TRNSYS modelling of the primary loop

The primary loop is one of the most difficult elements to model. In particular, unsteady phenomena in the solar field can lead to variations in the output steam flow. To our knowledge, there is no similar installation already studied. Thus, the originality of the studied solar micro-CHP unit prevents the use of model already existing in the TRNSys library. In order to implement the experimentally determined correlations and to have access to a database of the thermo-physical properties of water, Matlab© software has been used.

In Figure 9 the main Types used to model the primary circuit are shown. Between each of these Types, main information characteristics are the flow rate, enthalpy and pressure, which make it possible to carry out energy balances. The time schedule is the main control presented in green. The operating period of the micro-CHP unit is between 10h and 18h in order to benefit from the solar resource. It should be noted that the charging of the thermal storage tank is a determining factor in the control of the installation. Finally, the meteorological data, represented in blue, provide access to the evolution of sunshine and outdoor temperature according to the geographical location of the building. We consider in this study that it is located in La Rochelle, France. Note that Figure 9 shows an integration proposal for which the additional heat source (boiler) is located on the primary loop.

5.2 The secondary loop

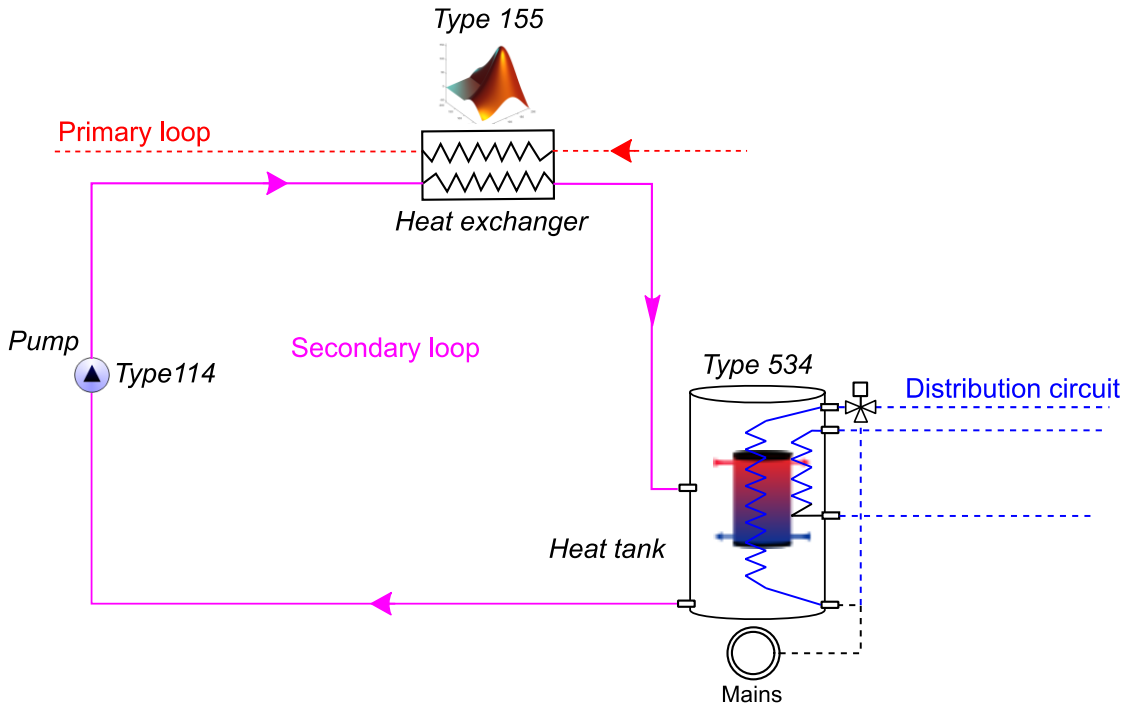

Figure 10: TRNSys modelling of the secondary loop

Figure 10 shows the secondary loop. Characteristics transmitted between the different types are mainly the flow rate, temperature and pressure of the water in the system.

Main parameters of this loop are the flowrate and storage tank characteristics. We considered a heat tank with two internal exchangers to meet the needs of the heating and DHW network.

5.3 The distribution loop and the coupling to the building

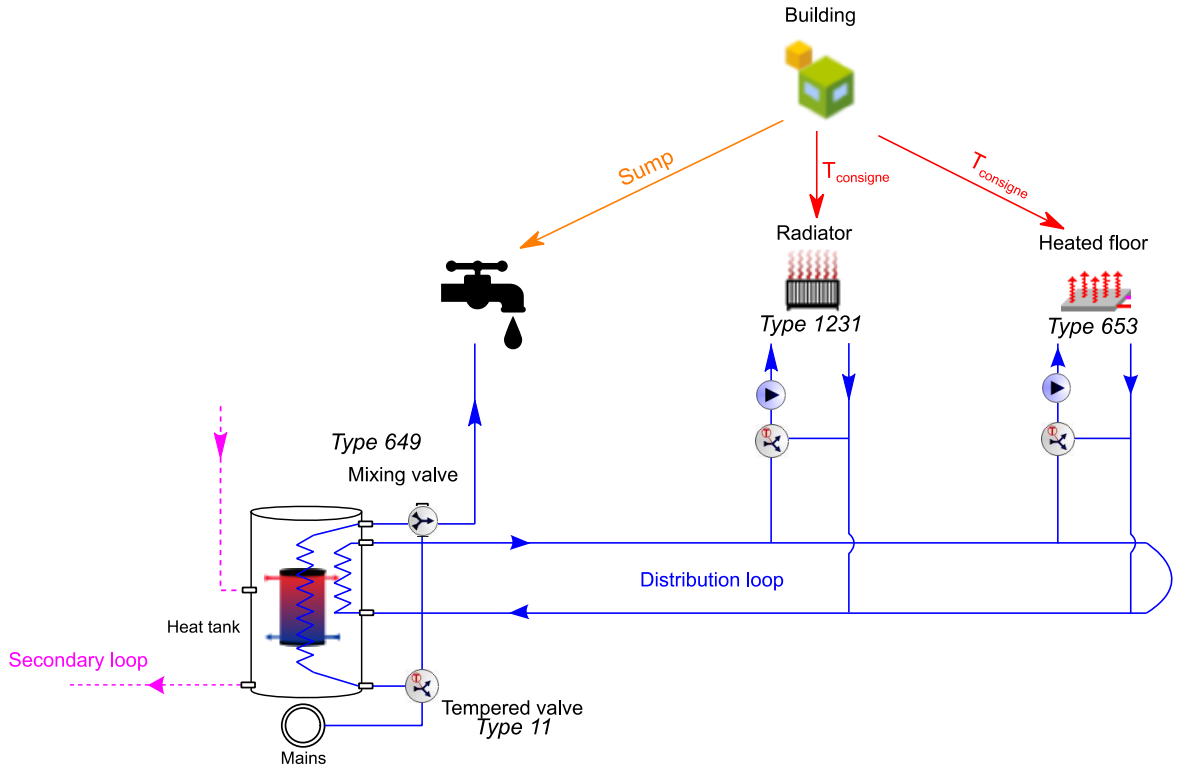

Figure 11: TRNSys modelling of the distribution loop

Finally, Figure 11 shows the distribution loop. For the DHW network, a tempering valve distributes the flow to the storage tank and to a mixing valve according to the set point temperature of 60 °C on the DHW withdrawal. It should be noted that heat losses located in the piping system were not taken in account here.

The pumps are located at the start of each hydraulic network. There are two heating networks in this installation: a radiator network composed by five radiators and a network for the underfloor heating. For clarity reasons, we represent only one radiator network in Figure 11.

For each emitter, tempering valves are used to adapt the supply temperature of the networks according to heating curve. The heating capacities are then injected into the building via the Type 56 in the form of gains for each zone of the building. The calculation of the thermal power emitted in each heated room takes into account its ambient temperature value.

5.3.1 Emitter modeling

The water regime of the radiators is determined in order to reach a temperature difference of 55/40 °C between inlet and outlet for outdoor conditions of -5 °C. The latter allows the sizing of emitters. For the underfloor heating system, the temperature difference between inlet and outlet is set to 35/28°C considering a flow rate of 120 kg/h.

It should be noted that a time schedule carries out the activation of the pump that supplies the radiator network, safety devices on the outside temperature and the ambient temperature. This means that the heating network is supplied according to a time schedule, but also if the outside temperature falls below -5 °C or if the ambient temperature in main rooms drops below 15 °C.

5.3.2 The distribution network

We detail in Figure 12 the radiator network operating principle. For underfloor heating, the control strategy is similar, without change in flowrate.

The achievement of the set point temperature in each room of the building is mainly ensured by:

- The flow temperature of the network, which is calculated using a heating curve depending on the outdoor temperature;
- The sizing of emitters, determined from usual laws;
- The flowrate control in each radiator, which is carried out by building occupants in practice, using thermostatic valves. A proportional flow control law based on the temperature difference between the set point and the ambient temperature was considered here. This law provides an opening signal in 0 and 1 calculated from the temperature difference between the ambient temperature and the set point (Figure 12).

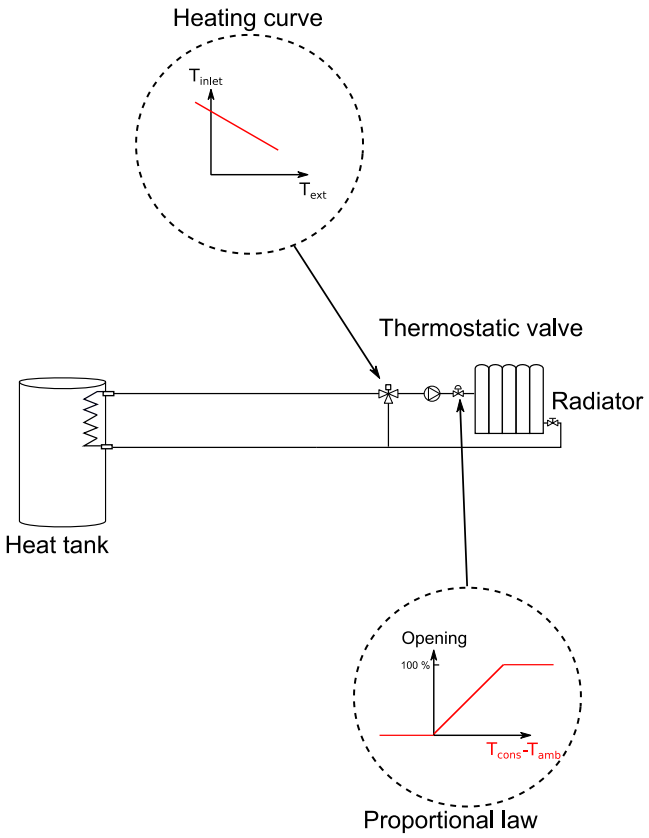

Figure 12: Schematic diagram of the radiator network

Thereafter, the radiator power is calculated by the emission law (12) and then taken into account in the heat balance of each heated room as a gain:

$$\dot{Q}_{radiator} = c(T_s - T_{amb})^n = \dot{m}C_p(T_{water,in} - T_{water,out}) \quad (12)$$

where c and n are constants depending on the type of radiator considered and the nominal operating conditions. The constant c is defined by the nominal conditions of operation while n corresponds to the type of radiator considered. For this simulation, the n value is equal to 1,4.

6. RESULTS

This section presents the main results from numerical simulations. For a week with heating needs (cold period), external conditions and powers generated by the micro-CHP units are plotted on Figure 13 and Figure 14 respectively. The weather data come from the Meteonorm database for the city of La Rochelle. Figure 14 confirms the need of an additional heat source (boiler) to ensure the continuous operation of the system.

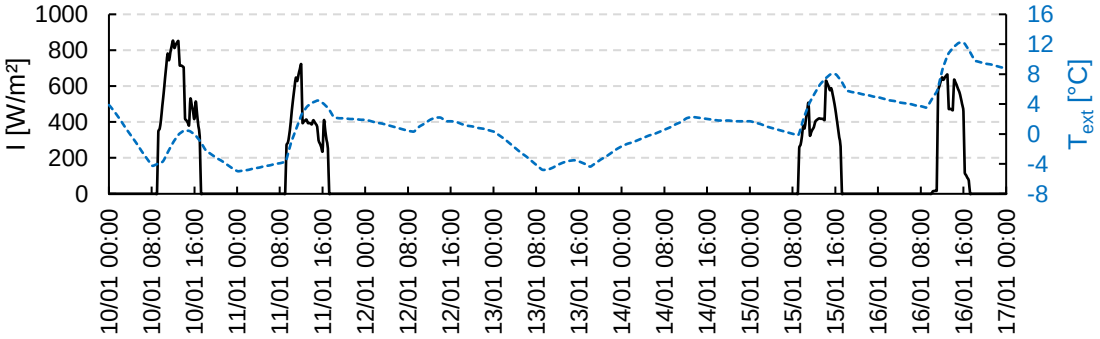

Figure 13: Evolution of solar irradiation and outside temperature

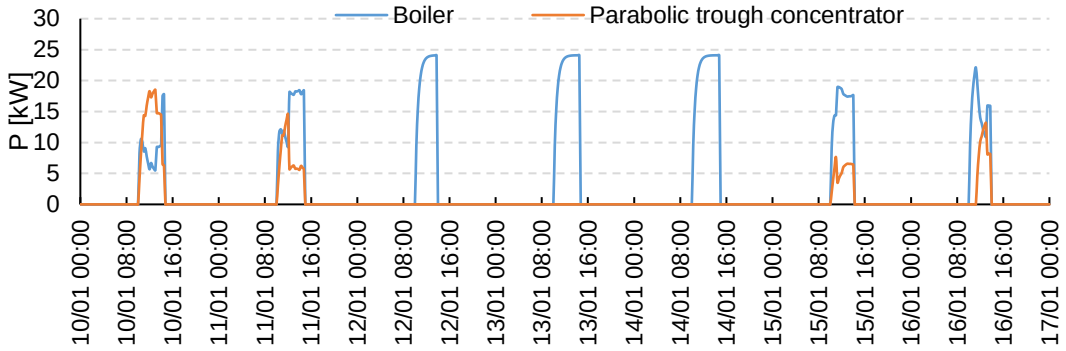

Figure 14: Evolution of the micro-CHP unit and boiler power

The boiler therefore supplements the concentrator's energy input and ensures constant inlet conditions to the steam engine. However, the system operation time is restricted by the storage tank load. Indeed, the micro-CHP unit is stopped while it is in its operating period. This is due to the fact that the average temperature of the storage tank has reached 85 °C. Figure 15 shows the evolution of the average temperature within the storage tank.

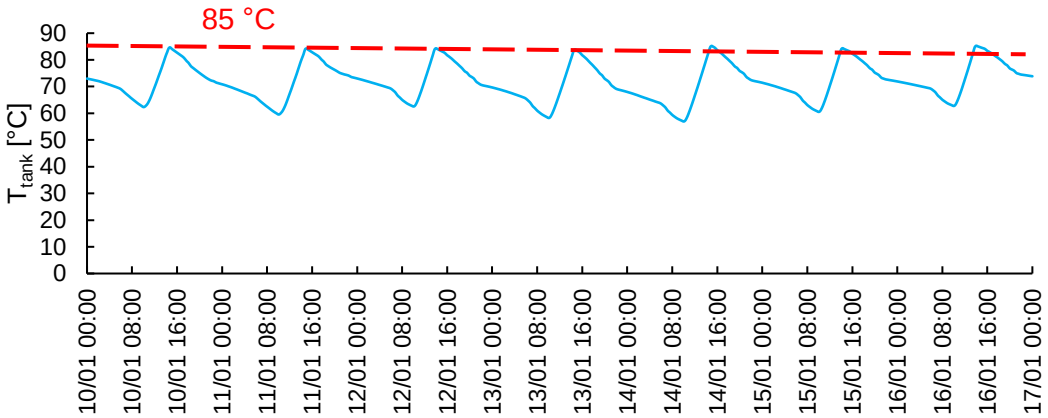

Figure 15: Average temperature within the storage tank

The average temperature in the storage tank must remain high enough to ensure temperature supply of domestic hot water, radiator and underfloor heating networks. The DHW and heating loads are presented by Figure 16.

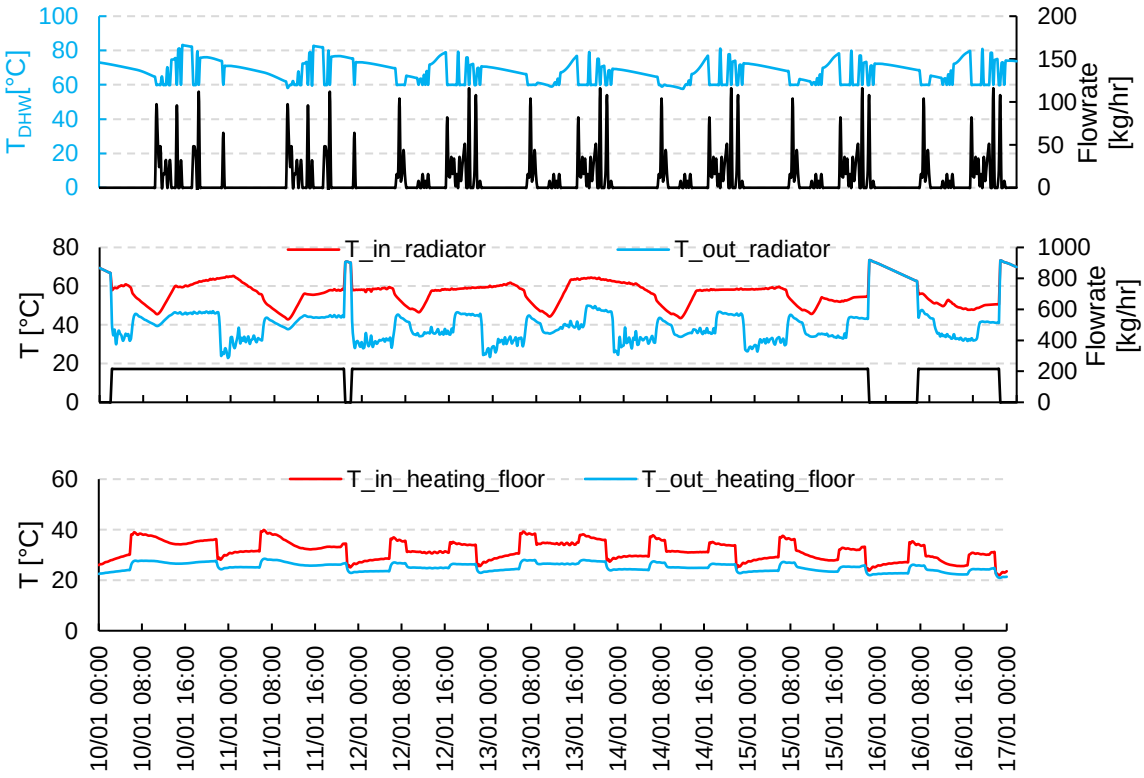

Figure 16: Details of the different water draws from the storage tank

The first graph in Figure 16 corresponds to the domestic hot water draws. The mixing valve outlet temperature is shown in blue. Thus, each time the withdrawal flow is not zero, this temperature must be equal to the set point temperature (60 °C). In other words, in order to meet the DHW requirements, the system must provide a temperature above 60 °C at the storage tank tap. The two others correspond to the radiator and underfloor heating network. For the radiators, a water regime of 55/40 °C for an outside temperature of -5 °C was chosen to determine the

network power. For the underfloor heating, a 35/28°C regime was chosen. The flow rate in the underfloor heating is constant, equal to 120 kg/hr.

Finally, power generation and consumption are shown by Figure 17. The superposition of these two curves makes it possible to quantify the self-consumed electricity as well as the electricity surplus and the imported electricity from the grid.

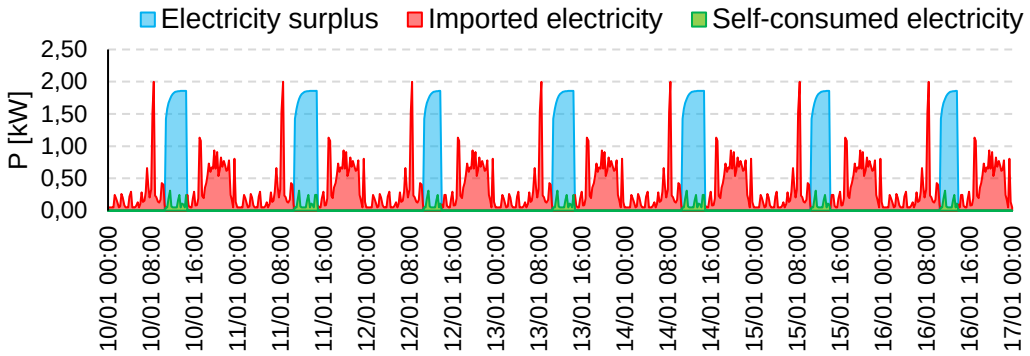

Figure 17: Electrical balance of the installation

Figure 17 points out the low self-consumption rate of the installation for the considered electricity consumption profile. Two observations can explain this low rate of electricity needs coverage. Firstly, the operation of the system between 10am and 6pm prevents production during the high evening demand. However, this is classical for solar systems. Secondly, it has already been mentioned that the system operation is limited by the storage tank load. Thus, the use of electrical storage and the increase in thermal requirements are two ways to improve performances of the micro-CHP unit. This second point will be discussed in section 8.

6.1 Summary

First of all an operating balance (illustrated by Figure 18) of the installation gives an account of the electrical and thermal energies produced by the installation from the energies consumed in order to obtain the output of the installation.

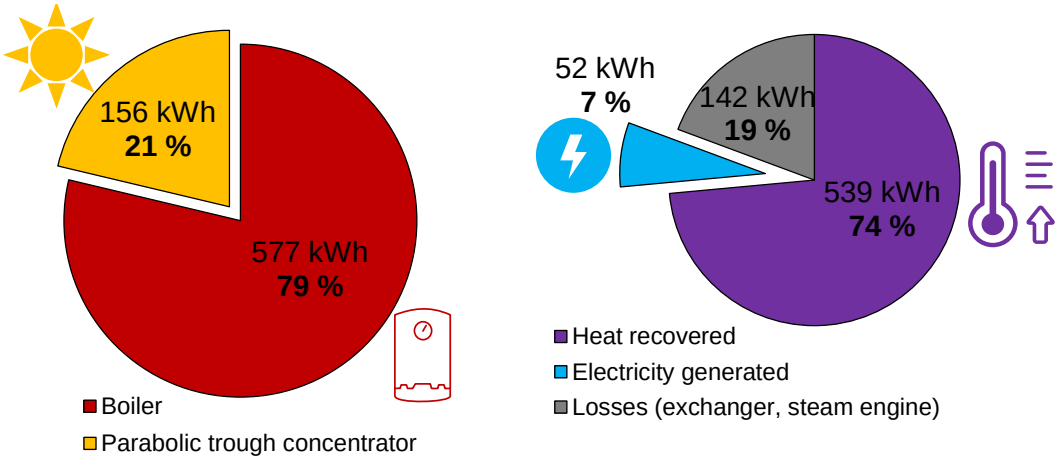

Figure 18: Balance of heat and electricity production by the micro-CHP unit for a cold week

During the heating period, the heating requirements are much higher than the requirements for DHW and electricity. The overall efficiency of the system is 81 % and it appears to be similar to that determined experimentally. A second assessment quantifies the final heat used by the consumer.

During the winter period heat needs are divided in DHW and heating needs. The latter is much greater than the first one, according to Figure 19. This was expected as in France, the DHW need represents 12.1% of the total average energy consumption, while it is 61.3% for heating [31].

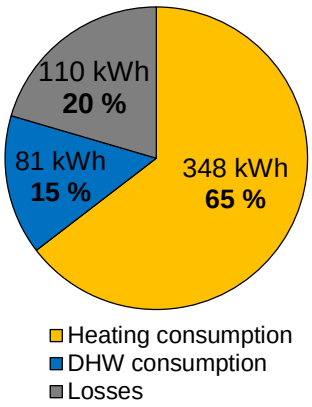

Figure 19: Balance of heat provided by the distribution loop

Finally, an overall assessment of the production by the micro-CHP unit has been carried out and shown by Figure 20. Note the importance of heat needs that represents 89% of the building's energy needs during the heating period.

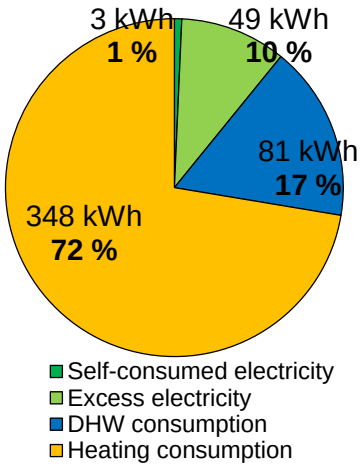

Figure 20: Balance of the production by the micro-CHP unit

6.2 Annual summary

For an entire year, production and consumption have been summed monthly and results are plotted in Figure 21. These results constitute an interesting synthesis of the operation of the micro-CHP unit during the whole year.

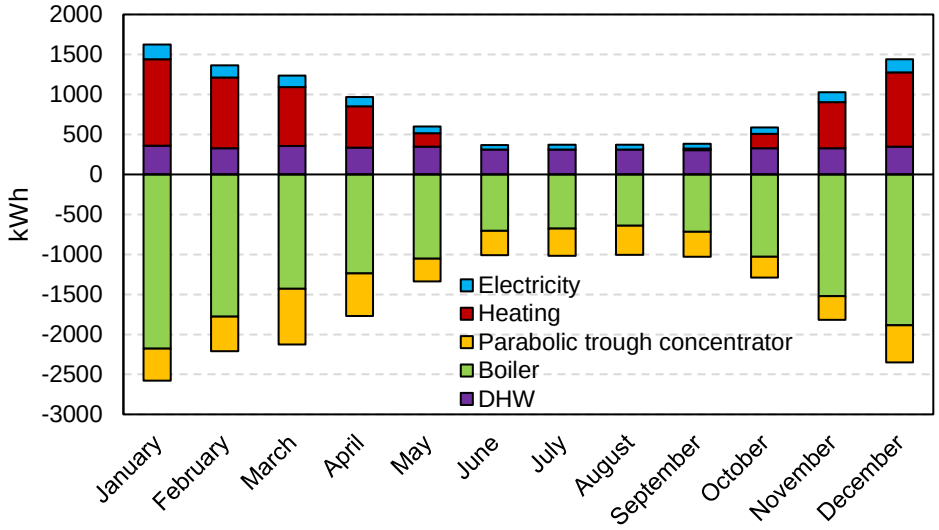

Figure 21: Balance of production and monthly consumption of the micro-CHP unit

It can be seen that DHW consumption remains constant while heating needs vary. Electricity is produced less in summer than in winter. This is due to the fact that the micro-CHP unit operates less in summer because it is limited by the load of the storage tank. Overall, the boiler's heat production remains majoritary in comparison to solar gains.

Finally, the overall efficiency decreases during the summer (63% in January and 37% in July). This is logical because the low heat consumption in summer means that the tank does not discharge much. Thus, the thermal losses of the storage tank are greater during the summer period.

7. IMPACT OF THE HEAT STORAGE VOLUME INCREASE ON THE SYSTEM PERFORMANCE

It has been shown that the charge of the storage tank is the limiting factor for the operation of the micro-CHP unit throughout the day. Indeed, the micro-CHP unit studied produces ten times more heat than electricity. It is therefore necessary to adapt the heat storage for such a system and we propose in this Section an investigation on the impact of the storage volume on its performance. For a whole year, we considered heat storage volumes ranging from 1 m^3 to 50 m^3 as shown by Figure 23.

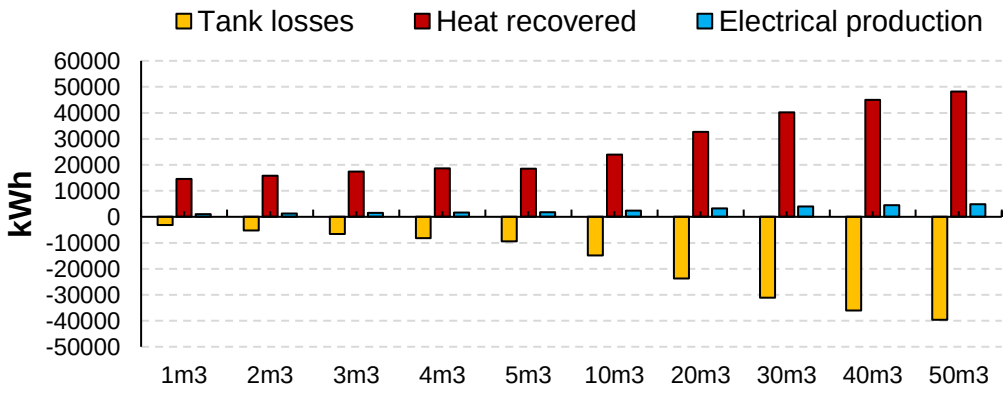

(a)

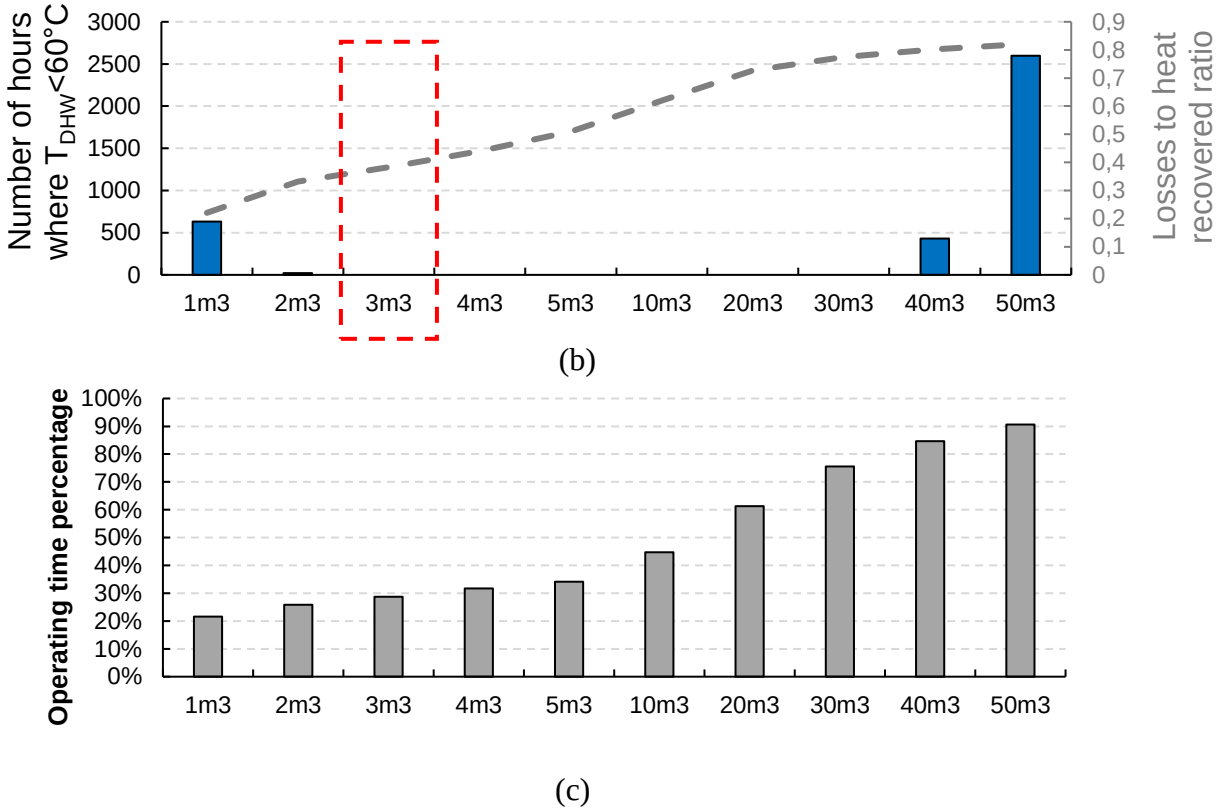

Figure 22: Effect of the heat storage volume on the system performance

Figure 23 points out that an increase in the storage volume has a small impact on the electrical production of the micro-CHP unit. A ten-fold increase in volume, from 1 to 10 m^3, leads to only a twofold rise in electrical production. A tank volume leading to the lowest loss ratio and ensuring heat requirements seems therefore to be the most relevant solution (Figure 23 (b)).

Not surprisingly, the system operating time is longer when the heat storage volume increases (20% of the maximum operating time for a volume of 1 m^3, 90% for a volume of 50 m^3). On one hand, such increase in heat storage volume leads to a more continuous operation but, on the other hand, it significantly increases heat losses.

The results suggest that preference should be given to the use of a 3 m^3 storage tank for this micro-CHP unit. To make the best use of the available heat, several houses with heat storage volumes could be connected. Indeed, low storage tanks volume limits heat losses while an increase in the number of consumers, and thus buildings, allows highest operating time of the system, and electricity production too.

8. CONCLUSIONS

In this article, we propose a solution for integrating a solar micro-CHP unit into a residential building. The system operates according to Hirn's thermodynamic cycle for electricity generation. It is based on direct steam generation within the absorber tube of a parabolic trough collector equipped with a two-axis solar tracking system.

Previous experimental works have pointed out the difficulty for the solar micro-CHP unit to operate without additional heater. We have therefore proposed a numerical model for integration of the micro-CHP unit to a building with backup on the primary loop.

Technically, the feasibility of adding such an additional heat source has to be studied. The results for a winter week and for a whole year show that the overall efficiency of the system can be interesting (up to 81 %). However, since it is oversized for a single building, it appears that its operation is limited by the storage tank load. An increase in the thermal load leads to an increase in the production by the system.

Finally, a parametrical study on the impact of the storage volume has been carried out. As the system produces a large amount of heat compared to its electrical production, it is necessary to propose an optimal heat use management strategy. Results suggest to share the heat between several dwellings with storage volumes of 3 m^3.

REFERENCES

[1] *Directive 2004/8/EC of the european parliament and of the council*.

[2] J.-B. Bouvenot, B. Latour, M. Siroux, B. Flament, P. Stabat, et D. Marchio, « Dynamic model based on experimental investigations of a wood pellet steam engine micro CHP for building energy simulation », *Applied Thermal Engineering*, vol. 73, nº 1, p. 1041- 1054, 2014.

[3] R. Beith, Éd., *Small and micro-combined heat and power (CHP) systems*. CRC Press, 2011.

[4] Anonymous, « 2030 climate & energy framework », *Climate Action - European Commission*, 23-nov-2016. [En ligne]. Disponible sur: https://ec.europa.eu/clima/policies/strategies/2030_en. [Consulté le: 19-sept-2018].

[5] S. Martinez, G. Michaux, P. Salagnac, et J.-L. Bouvier, « Micro-combined heat and power systems (micro-CHP) based on renewable energy sources », *Energy Conversion and Management*, vol. 154, p. 262- 285, 2017.

[6] J.-L. Bouvier, G. Michaux, P. Salagnac, F. Nepveu, D. Rochier, et T. Kientz, « Experimental characterisation of a solar parabolic trough collector used in a micro-CHP (micro-cogeneration) system with direct steam generation », *Energy*, vol. 83, p. 474- 485, 2015.

[7] J.-L. Bouvier, G. Michaux, P. Salagnac, T. Kientz, et D. Rochier, « Experimental study of a micro combined heat and power system with a solar parabolic trough collector coupled to a steam Rankine cycle expander », *Solar Energy*, vol. 134, p. 180- 192, 2016.

[8] J.-L. Bouvier, V. Lemort, G. Michaux, P. Salagnac, et T. Kientz, « Experimental study of an oil-free steam piston expander for micro-combined heat and power systems », *Applied Energy*, vol. 169, nº Supplement C, p. 788- 798, 2016.

[9] J.-L. Bouvier, « Étude expérimentale d'une installation de micro-cogénération solaire couplant un concentrateur cylindro-parabolique et un moteur à cycle de Hirn », Thèse de doctorat, La Rochelle, 2014.

[10] Á. Campos-Celador, E. Pérez-Iribarren, J. M. Sala, et L. A. del Portillo-Valdés, « Thermoeconomic analysis of a micro-CHP installation in a tertiary sector building through dynamic simulation », *Energy*, vol. 45, nº 1, p. 228- 236, sept. 2012.

[11] Y. Lebbe et D. Darimont, « Réussir l'intégration de l'hydraulique et de la régulation d'une cogénération dans une chaufferie », Guide technique, 2014.

[12] X. P. Chen, N. Hewitt, Z. T. Li, Q. M. Wu, X. Yuan, et T. Roskilly, « Dynamic programming for optimal operation of a biofuel micro CHP-HES system », *Applied Energy*, vol. 208, p. 132- 141, déc. 2017.

[13] M. A. Rosen, M. N. Le, et I. Dincer, « Efficiency analysis of a cogeneration and district energy system », *Applied Thermal Engineering*, vol. 25, n° 1, p. 147- 159, janv. 2005.

[14] V. Havelský, « Energetic efficiency of cogeneration systems for combined heat, cold and power production », *International Journal of Refrigeration*, vol. 22, n° 6, p. 479- 485, sept. 1999.

[15] T. Nuytten, B. Claessens, K. Paredis, J. Van Bael, et D. Six, « Flexibility of a combined heat and power system with thermal energy storage for district heating », *Applied Energy*, vol. 104, p. 583- 591, avr. 2013.

[16] S. Sanaye, M. A. Meybodi, et S. Shokrollahi, « Selecting the prime movers and nominal powers in combined heat and power systems », *Applied Thermal Engineering*, vol. 28, n° 10, p. 1177- 1188, juill. 2008.

[17] A. Williams, « Micro-CHP in buildings », *Build Up*, 21-juin-2011. [En ligne]. Disponible sur: http://www.buildup.eu/en/topics/micro-chp-buildings. [Consulté le: 19-sept-2018].

[18] « Cogeneration of heat and power - Energy - European Commission », *Energy*. [En ligne]. Disponible sur: /energy/en/topics/energy-efficiency/cogeneration-heat-and-power. [Consulté le: 19-sept-2018].

[19] H. I. Onovwiona et V. I. Ugursal, « Residential cogeneration systems: review of the current technology », *Renewable and Sustainable Energy Reviews*, vol. 10, n° 5, p. 389- 431, oct. 2006.

[20] « European and Canadian non-HVAC electric and DHW load profiles for use in simulating the performance of residential cogeneration systems[A report of Subtask A of FC+COGEN-SIM : The simulation of building-integrated fuel cell and other cogeneration systems : Annex 42 of the International Energy Agency, Energy Conservation in Buildings and Community Systems Programme] (Book) | ETDEWEB ». [En ligne]. Disponible sur: https://www.osti.gov/etdeweb/biblio/20987338. [Consulté le: 19-sept-2018].

[21] M. Dentice d'Accadia, M. Sasso, S. Sibilio, et L. Vanoli, « Micro-combined heat and power in residential and light commercial applications », *Applied Thermal Engineering*, vol. 23, n° 10, p. 1247- 1259, juill. 2003.

[22] R. J. Braun, S. A. Klein, et D. T. Reindl, « Evaluation of system configurations for solid oxide fuel cell-based micro-combined heat and power generators in residential applications », *Journal of Power Sources*, vol. 158, n° 2, p. 1290- 1305, août 2006.

[23] A. D. Hawkes et M. A. Leach, « Cost-effective operating strategy for residential micro-combined heat and power », *Energy*, vol. 32, n° 5, p. 711- 723, mai 2007.

[24] S. A. Kalogirou, « Solar thermal collectors and applications », *Progress in Energy and Combustion Science*, vol. 30, n° 3, p. 231- 295, 2004.

[25] S. Bendapudi, J. E. Braun, et E. A. Groll, « A comparison of moving-boundary and finite-volume formulations for transients in centrifugal chillers », *International Journal of Refrigeration*, vol. 31, n° 8, p. 1437- 1452, déc. 2008.

[26] E. Zarza *et al.*, « Direct steam generation in parabolic troughs: Final results and conclusions of the DISS project », *Energy*, vol. 29, n° 5–6, p. 635- 644, 2004.

[27] M. Eck et T. Hirsch, « Dynamics and control of parabolic trough collector loops with direct steam generation », *Solar Energy*, vol. 81, n° 2, p. 268- 279, 2007.

[28] R. Xu et T. F. Wiesner, « Closed-form modeling of direct steam generation in a parabolic trough solar receiver », *Energy*, vol. 79, p. 163- 176, janv. 2015.

[29] S. Quoilin, V. Lemort, et J. Lebrun, « Experimental study and modeling of an Organic Rankine Cycle using scroll expander », *Applied Energy*, vol. 87, n° 4, p. 1260- 1268, avr. 2010.

[30] E. McKenna et M. Thomson, « High-resolution stochastic integrated thermal–electrical domestic demand model », *Applied Energy*, vol. 165, p. 445- 461, 2016.

[31] ADEME, « L'eau chaude sanitaire », *ADEME*. [En ligne]. Disponible sur: https://www.ademe.fr/expertises/batiment/passer-a-laction/elements-dequipement/leau-chaude-sanitaire. [Consulté le: 06-août-2018].